COMMUNICATION

On the Efficiency Limit of Conjugated Polymer:Fullerene-Based Bulk Heterojunction Solar Cells

Markus C. Scharber*

Harvesting the almost unlimited solar radiation provided by the sun to produce electricity is one of the most promising solutions for the world's energy demands. Today silicon-based, the so-called first generation, solar cells dominate the market. Their excellent proven performance and their relatively low cost make them the first choice for energy-harvesting applications on roofs or via the ground-mounted power plants. However, there has been an intensive search for alternative photovoltaic devices since the development of the first solar cells in the 1950s. Lower manufacturing costs, higher power conversion efficiencies, and applications not suitable for the silicon solar cells have been the main drivers for exploring alternative semiconducting absorbers. Bulk heterojunction (BHJ) organic photovoltaic cells (OPV) possess several advantages over inorganic silicon-based devices such as simple manufacturing, the possibility of large-scale roll-to-roll production by solution-processing techniques, lower manufacturing cost, and the ability to provide flexible, low-weight, and semitransparent photovoltaic material.

The power conversion efficiency of BHJ cells made from blends of conjugated polymers and soluble fullerene derivatives has increased from around 1% to over 11% in the past 15 years. The evolution of certified PCEs reported in the efficiency tables published in Progress in Photovoltaics is summarized in **Figure 1**.[1] Efficiency tables also contain a section with the so-called "Notable Exception"—referring to solar cells with an area smaller than 1 cm². Their development is plotted in Figure 1 (dots) as well. The first data point in Figure 1 refers to an externally verified efficiency reported by Shaheen et al.[2] The first certified data, measured on a 3% efficient poly-3-hexyl-thiopehene (P3HT)—[6,6]-phenyl-C_{61}-butyric acid methyl ($PC_{60}BM$) device fabricated by Sharp, were published in Progress in Photovoltaics in 2006 (Efficiency Table 28).[3] In the same year the paper "Design Rules for Donors in Bulk Heterojunction Solar Cells—Towards 10% Energy-Conversion Efficiency" was published in Advanced Materials.[4] In the remaining part of the manuscript, Reference 4 will be referred to as AM2006. The experimental data and the model summarized a systematic material screening effort performed at Konarka Austria in 2003. Based on in depth electrochemical characterization followed by an optimization of the solar cell performance an empirical equation for the open-circuit voltage

(V_{oc}) of BHJ devices was derived. For these studies all polymers were mixed with the fullerene acceptor $PC_{60}BM$.

Experimental data presented in AM2006 are replotted in **Figure 2**. In addition, new data points are added (stars) for the conjugated polymers investigated in the current study. From a linear fit one finds that the V_{oc} can be extrapolated by $1/q$ (q is the unit charge) times the position of the highest occupied molecular orbital (HOMO) level of the donor minus 4.6 V. By assuming a fill factor of 65% and a constant external quantum efficiency (EQE) of 65% for photon energies larger than the bandgap of the donor polymer the power conversion efficiency of a BHJ solar was calculated as a function of the bandgap and the HOMO level of the donor polymer. The resulting contour plot—sometimes called the "Scharber-diagram" or "Scharber-plot"—proposes an ideal bandgap and the position of the HOMO level of the donor.[5] The findings presented in AM2006 have had an enormous impact on the development efforts of new absorber materials within the OPV community. Many chemists used the proposed guidelines to design new semiconductors with higher performance potential.[6,7] The simple model was also applied to evaluate the compounds analyzed by means of quantum chemical calculations within the "Clean Energy Project" initiated by Harvard University.[8,9]

While the position of energy levels determines the maximum efficiency, it was found that the molecular arrangement of the donor polymer and the acceptor—often referred to as nanomorphology—limits the performance of a majority of studied materials.[10] On the one hand, the donor–acceptor arrangement should enable efficient charge transport—which would require large, pure donor and acceptor volumes. On the other hand, large donor–acceptor interfaces are important for efficient exciton dissociation—which requires mixing of the donor and acceptor moieties on a molecular level. The ideal nanomorphology was found to be an interpenetrating bicontinuous network of donor-rich and acceptor-rich domains with sizes on the 20–40 nm length scale.[11] Despite very intensive research, today it is not possible to precisely predict the nanomorphology of conjugated polymer—fullerene blends. Thermodynamics suggests that the degree of intermixing is determined by the minimum of the free energy of the system, which comprises the entropy and the enthalpy. The entropy term favors a complete mixing of the donor and acceptor on a molecular level. The enthalpic term could decrease or increase upon mixing, depending on the interaction energies between donor and acceptor molecules. However, morphologies found in high-performance bulk heterojunction solar cells are often thermodynamically metastable as they were formed during the rapid solidification of a thin wet layer deposited on a substrate and the simple equilibrium thermodynamic arguments may

Dr. M. C. Scharber
Linz Institute for Organic Solar Cells
Johannes Kepler University Linz
Altenbergerstrasse 69, 4040 Linz, Austria
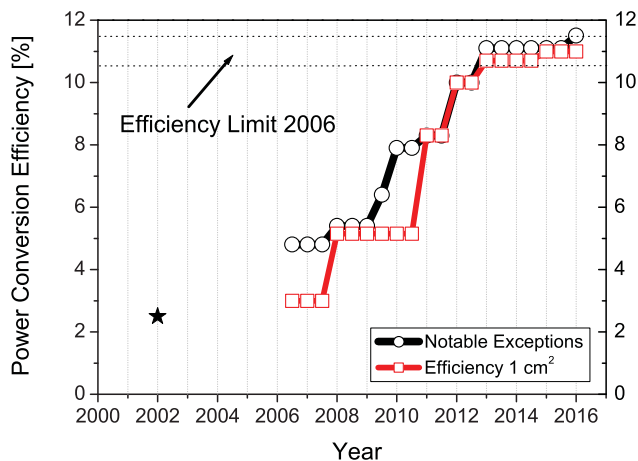E-mail: Markus_Clark.Scharber@jku.at

Figure 1. Development of the power conversion efficiency of organic solar cells.

not be appropriate for explaining the resulting morphology. Therefore, the optimization of the donor–acceptor arrangement on a molecular level has been trial-and-error based. Today several different techniques are available, which allow altering the nanomorphology of organic solar cell absorber layers. Chemists have applied different side chains and selective substitutions, especially using fluorine, to tune the miscibility of donor and acceptor materials.[12,13] In addition, the selection of solvents or solvent mixtures,[14] the use of processing additives like alkane-dithiols,[15] the annealing of films at elevated temperatures,[16] or using solvent vapor[17] was found to be useful for optimizing the nanomorphology. With all this tricks and conjugated polymers with a favorable bandgap and HOMO-position, efficiencies up to 11% have been reported[18]—a value already very close to the efficiency limit proposed in AM2006.

Comparing PCEs of best inorganic and organic solar cells one finds that, besides slightly lower electrical fill factor and external quantum efficiencies, organic solar cells suffer from a
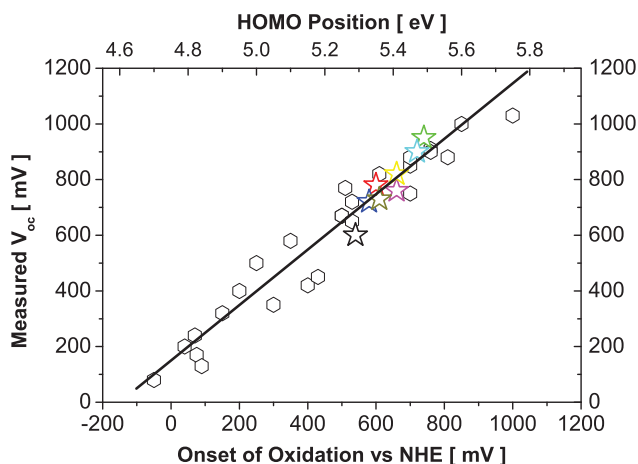
large open-circuit voltage loss.[19] When operated under 1 sun illumination—the energy loss E_{loss} defined by $E_g - qV_{oc}$ with E_g being the bandgap of the semiconductor, q is the unit charge and V_{oc} is the open-circuit voltage of the solar cell—is ≈0.3 eV for a GaAs solar cell prepared by Alta Devices (PCE ≈ 29%) (V_{oc} = 1,12 V, E_g ≈ 1.4 eV). Under the same conditions, the most efficient OPV (Toshiba, PCE ≈ 11%) with a bandgap of ≈1.5 eV delivers an open-circuit voltage of 0.79 V resulting in an E_{loss} ≈0.7 eV.[18] The origin for the huge voltage loss has been investigated extensively. Rapid recombination of photoinduced charges in the absorber bulk or at the semiconductor electrode or pinning of the electrodes to states in the bandgap has been discussed as possible sources for the observed loss.[20,21] After the discovery of the charge-transfer state (CTS) sometimes also called charge-transfer complex or charge-transfer exciton, formed between the donor polymer and the acceptor, this new species moved into the focus of the OPV loss analysis.[22,23] The CTS was first observed as weak emission in electroluminescence experiments on MEH–PPV (poly[2-methoxy-5-(2-ethylhexyloxy)-1,4-phenylenevinylene])—PC$_{60}$BM blends.[24] The CTS absorption was first detected by measuring the EQE of an MDMO-PPV (poly[2-methoxy-5-(3′,7′-dimethyl-octyloxy)]-p-phenylene-vinylene):PC$_{60}$BM solar cell. Using Fourier-transform photocurrent spectroscopy, Goris et al.[25] found a very small photocurrent signal in a spectral range where neither the donor polymer nor the acceptor fullerene absorbs. In these early publications, the weak absorptions and emissions were not assigned to transitions in a CTS but to defect states or direct transitions between the donor and the acceptor levels. In 2007, Benson-Smith et al.[26] and Loi et al.[27] reported their observations of a CTS in polyfluorene-based donor and fullerene acceptor blends. These reports initiated extensive investigations of the impact of the CTS on the photovoltaic properties of BHJ. A linear relation between the open-circuit voltage and the energy of the CTS was found for many different donor–acceptor couples.[28] The CTS was identified as an important recombination center leading to predominantly nonradiative recombination of electrons and holes.[29] These observations combined with the reciprocity relation[30] between photovoltaic quantum efficiency and electroluminescence of solar cells were used by Vandewal et al.[23] to rationalize the large open-circuit voltage loss in OPVs. Further analysis suggested that the CTS formed between donor and acceptor in organic solar cells is ultimately limiting the power conversion efficiency of this type of devices.[31] The weak absorption of the CTS lowers the effective bandgap of the photovoltaic cell but makes only a very small contribution to the photocurrent current. The low radiative recombination quantum yield of CTS is reducing the V_{oc} further leading to the observed ≈1 V loss. The overall effect of the CTS energetic position and the oscillator strength on the power conversion efficiency has been analyzed by several authors. Applying thermodynamic arguments, the detailed balance approach proposed by Shockley and Queisser or the reciprocity relation by Rau, calculations showed that a very weak or a very strong absorption of the CTS does lead to the highest PCE.[32,33] Based in these findings several author estimated the ultimate PCE of OPVs. They found that under ideal conditions (increasing the radiative recombination quantum yield and optimizing the energetic and optical properties of the CTS)

Figure 2. Open-circuit voltage (V_{oc}) of different bulk heterojunction solar cells plotted versus the oxidation potential/HOMO position of the donor polymer used in each individual device. Open circles are taken from AM2006, stars represent different polymers investigated in this study. The straight line represents a linear fit with a slope of 1.

OPVs could be as efficient as the best inorganic photovoltaic devices.

Recently, several different new conjugated polymers have been reported giving efficiencies in the range of 9%–11% when blended with suitable fullerene acceptors.[34–36] In this manuscript, the electrochemical, electrical, and optical characterization of eight selected high-performance polymers is described. The overall goal of this work was the investigation of the losses limiting the power conversion efficiency of devices made of the selected semiconductors. Experimental data are analyzed following the model proposed in AM2006. It is found that all investigated polymers form CTS with the fullerene acceptor PCBM. Solar cells exhibit typical V_{oc} losses and a weak low energy absorption and emission can be observed in the EQE and electroluminescence spectra, respectively. All results suggest that even the best performing bulk heterojunction devices suffer from typical losses observed in state-of-the-art OPVs. High power conversion efficiencies are achieved by optimizing of the bandgap and the energy levels as proposed in AM2006 and the nanomorphology of the polymer–fullerene blends enabling efficient charge separation and excellent charge transport at the same time. None of the investigated absorber blends showed more favorable CTS absorption or enhanced radiative recombination. All this suggests that even the most efficient OPVs are essentially limited by the basic design rules proposed in AM2006.

In **Figure 3**, the chemical structures of the investigated polymers are shown. Materials were used as received without any further purification. Absorption and photoluminescence spectra of thin polymer films deposited on glass substrates are shown in Figure S1 (Supporting Information).

In **Figure 4**, the onsets of the first electrochemical oxidation determined with electrochemical–voltage spectroscopy (EVS)[43] of all polymers are plotted.

The polymer PBDTTPD showed some tendency to peel off the platinum electrode during the electrochemical experiment. Despite applying the EVS method, the integrated charge versus applied voltage curves of most of the polymers exhibits a small slope between 0 V and the onset of the oxidation. This suggests that a small amount of impurities may be present in the different polymer samples. The extracted HOMO levels of the different materials are summarized in **Table 1**.

The calculated[4] and measured open-circuit voltages of corresponding BHJ solar cells are listed as well for comparison. Measured data points are also plotted in Figure 2. All polymers follow the linear relation between the open-circuit voltage and the position of the donor HOMO level, which was found earlier for many different BHJ solar cells. Typical performance data of prepared solar cells measured on a solar simulator are shown in **Table 2**. Devices were processed following the recipes described in literature.[34,35,38–42] All solar cells show typical open-circuit voltages and electrical fill factors (FF). Due to the
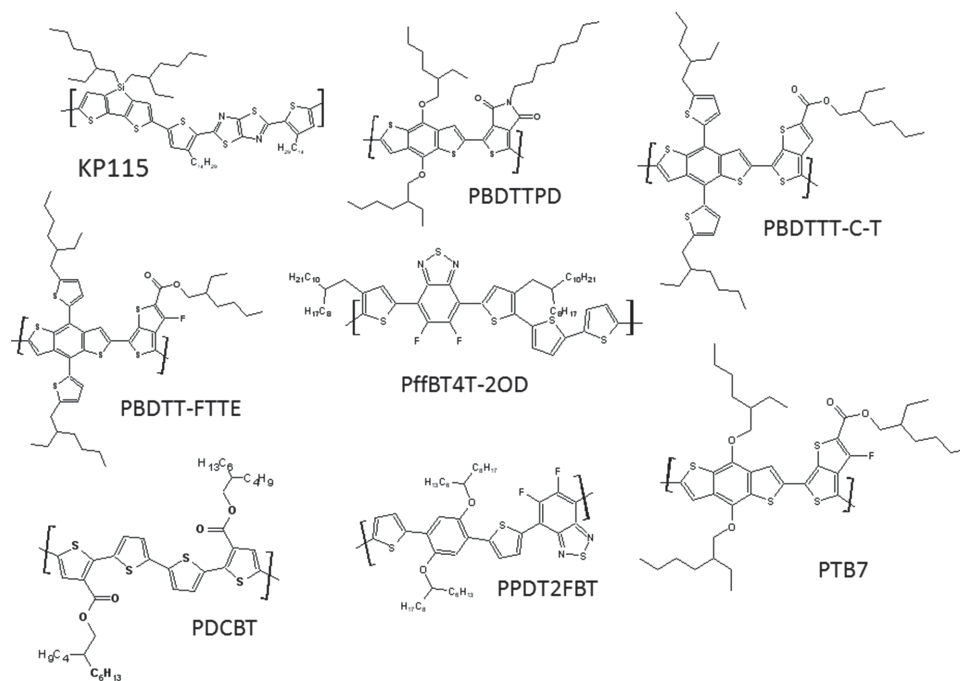

Figure 3. Chemical structure of investigated polymers: KP115 (poly[(4,4′-bis (2-ethylhexyl) dithieno [3,2-b:2′,3′-d] silole)-2,6-diyl-alt-(2,5-bis 3-tetradecylth-iophen-2-yl-thiazolo-5,4-d-thiazole)-2,5diyl],[37] PBDTTPD (poly[[5-(2-ethylhexyl)-5,6-dihydro-4,6-dioxo-4H-thieno[3,4-c]pyrrole-1,3-diyl][4,8-bis[(2-ethylhexyl)oxy]benzo[1,2-b:4,5-b']dithiophene-2,6-diyl]]),[38] PBDTTT-C-T (2,6-bis(trimethyltin)-4,8-bis(5-(2-ethylhexyl)thiophen-2-yl)benzo[1,2-b:4,5-b']-dithiophene),[39] PBDTT-FTTE (poly[4,8-bis(5-(2-ethylhexyl)thiophen-2-yl)benzo[1,2-b;4,5-b']dithiophene-2,6-diyl-alt-(4-(2-ethylhexyl)-3-fluorothieno[3,4-b]thiophene-)-2-carboxylate-2-6-diyl])),[35] PffBT4T-2OD (poly[(5,6-difluoro-2,1,3-benzothiadiazol-4,7-diyl)-alt-(3,3′′′-di(2-octyldodecyl)-2,2′;5′, 2′′;5′′,2′′′-quaterthiophen-5,5′′′-diyl)]),[34] PDCBT (poly[5,5′-bis(2-butyloctyl)-(2,2′-bithiophene)-4,4′-dicarboxylate-alt-5,5′-2,2′-bithiophene]),[40] PPDT2FBT (poly[(2,5-bis(2-hexyldecyloxy)phenylene)-alt-(5,6-difluoro-4,7-di(thiophen-2-yl)benzo[c]-[1,2,5]thiadiazole)]),[41] PTB7 (poly({4,8-bis[(2-ethylhexyl)oxy]-benzo[1,2-b:4,5-b']dithiophene-2,6-diyl}{3-fluoro-2-[(2-ethylhexyl)carbonyl]thieno[3,4-b]thiophenediyl})).[42]
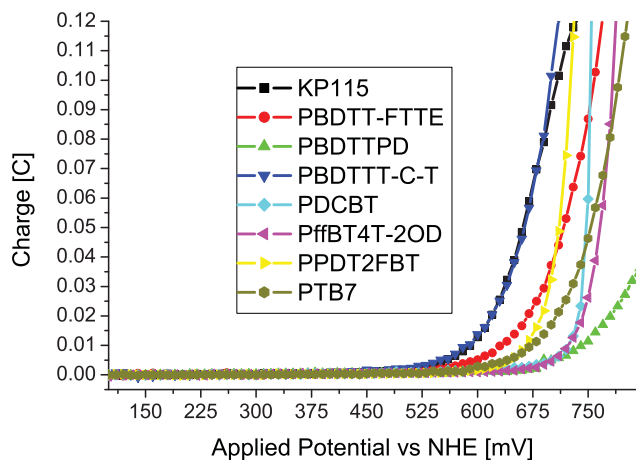
Figure 4. EVS measurements for oxidation of different polymers.

Table 2. Device parameter of different BHJ-solar cells.

Polymer	V_{oc} [V]	I_{sc} [mA cm^{-2}]	FF [%]	Efficiency [%]
KP115	0.61	10.47	67.4	4.3
PBDTT–FTTE	0.78	10.71	64.0	5.3
PBDTTPD	0.95	4.39	64.2	2.7
PBDTTT-C-T	0.72	7.59	60.0	3.3
PDCBT	0.90	10.39	67.6	6.4
PffBT4T-2OD	0.77	13.47	70.4	7.3
PPDT2FBT	0.82	11.19	71.1	6.5
PTB7	0.73	10.00	65.0	4.7

use of PC$_{60}$BM and not optimized layer thicknesses the short-circuit currents are lower compared to best reported values.

In addition to standard bulk heterojunction solar cells based on polymer–fullerene blends, also devices with polymer absorber layers or a pure PC$_{60}$BM absorber layer were prepared. These devices show very low photocurrents when measured under solar radiation. However, when operated as light emitting diodes, most of them show strong electroluminescence. (see Figure S2, Supporting Information). **Figure 5**a compares the EQE spectra of and single absorber diodes including one with a PC$_{60}$BM absorber layer.

For all investigated polymer diodes expect the one with KP115 as a absorber, a steep onsets in the EQE spectra are found. The KP115 diode shows a low energy tail suggesting that impurities forming states in the gap of the polymer are present. EQE spectra can be used to estimate the onset of absorption of the materials (see Table S1, Supporting Information). For comparison also the position of the photoluminescence maximum and the absorption onset estimated from the absorbance spectra are listed.

External quantum efficiency spectra of the prepared BHJ solar cells are plotted in Figure 5b. The EQE are substantially higher than the polymer-only diodes and show the characteristic low energy contribution, which is assigned to the CTS. Figure 5c compares the EQEs of a PPDT2FBT-based diode and

Table 1. HOMO levels of different polymers, measured and calculated open-circuit voltages of BHJ solar cells.

Polymer	HOMO level [eV]	V_{oc} [V] predicted according to AM2006	V_{oc} [V] measured
KP115	−5.29	0.69	0.61
PBDTT-FTTE	−5.35	0.75	0.78
PBDTTPD	−5.49	0.89	0.95
PBDTTT-C-T	−5.33	0.73	0.72
PDCBT	−5.47	0.87	0.9
PffBT4T-2OD	−5.41	0.81	0.77
PPDT2FBT	−5.41	0.81	0.82
PTB7	−5.36	0.76	0.73

the corresponding BHJ solar cell. The onset of the EQE of the BHJ device is shifted by about 0.3 eV to lower photon energies compared to the polymer diode. KP115:PCBM solar cells show the most pronounced low energy absorption feature. This may be related to the impurities observed in the pristine polymer, which transfer an electron to the fullerene acceptor upon photoexcitation as well. The EQE spectra of the different BHJ-solar cells can also be used to estimate the energetic position of the charge-transfer state (E_{CT}) and the open-circuit voltage of the devices. For the investigated absorber materials, a good correlation between V_{oc} and E_{CT} is found (Figure S3, Supporting Information).

Another experiment to test the presence of a CTS is operating the solar cells as LEDs, i.e., by injecting charge carriers under forward bias. The injected carriers recombine in the semiconductor and, in many cases, a low energy emission different from the EL of the donor polymer or the acceptor fullerene is observed. The CTS emission is usually very weak and can be hidden in the residual emission resulting from a recombination of electrons or holes on donor or acceptor molecules. Also an unfavorable nanomorphology or energetically lower lying molecular states (e.g., triplet) may reduce the recombination of charges through the CTS in the investigated heterojunction systems.[22,44] In **Figure 6**, the electroluminescence spectra of a PDCBT-diode and a PCBDT:PC$_{60}$BM bulk heterojunction solar cell are compared. The emission of the BHJ was recorded using a cooled silicon CCD (red) and an InGaAs diode array (green).

All BHJ–EL spectra were recorded at moderate forward bias voltages (1–1.4 V). In some cases, the emission originating from the polymer started to dominate the recorded signal at higher voltages. The CTS emission intensity is three to four orders of magnitudes smaller compared to the electroluminescence of the polymer-only diode. The spectra in Figure 6 are scaled to comparable amplitudes for better visibility. Spectra for the other semiconductors are shown in Figure S4 (Supporting Information).

Using the data above and the model (AM2006), the performance potential of the investigated materials can be determined. As many high-performance BHJ solar cells fabricated today show electrical fill factors (FF) and quantum efficiencies (EQE) in the range of 70%, a FF = 70% and an average EQE of 70% are assumed for the performance calculations. For the original calculations, a value of 0.65 was used for the FF and EQE. Results are summarized in **Figure 7**. In the contour plot, the power conversion efficiency is plotted versus the absorption
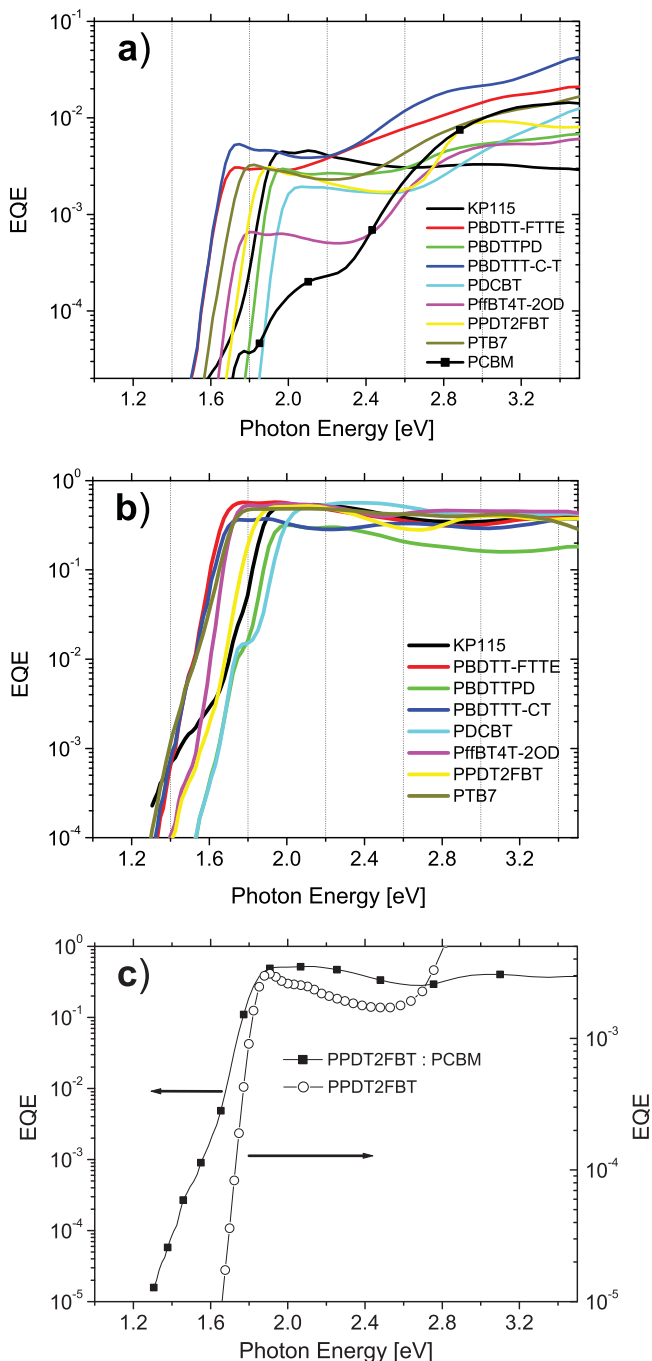
**ADVANCED
MATERIALS**
www.advmat.de

COMMUNICATION

Materials Views
www.MaterialsViews.com

Figure 6. Electroluminescence spectra of a PDCBT-diode (black), a PDCBT:PCBM solar cell recorded with a Si-CCD (red) and an InGaAs-detector array (green).

The findings presented above suggest that all investigated polymers suffer from typical losses found for many other BHJ solar cells. The simple model used to estimate performance potential is accounting for all observed losses properly. The good agreement between the position of the donor HOMO level and the observed V_{oc} illustrates that all solar cells show typical ≥700 mV loss in the open-circuit voltage. The presence of the weakly absorbing/emitting CTS supports the idea that all studied BHJs are limited by the energetics and recombination processes within the CTS. These findings also support the idea that AM2006 model is applicable to the investigated polymers and that the power conversion efficiency is limited to approximately 13%. A recent study published by the Janssen and co-workers[45] suggests that organic semiconductors with optimized energy levels will not reach highest efficiencies. A literature survey combined with their own experimental data revealed that solar cells exhibiting an energy loss E_{loss} < 700 mV do not reach high external quantum efficiencies (<70%). In case this empirical finding turns out to be an intrinsic property of

Figure 5. a) EQE spectra of polymer diodes and one device with a PC$_{60}$BM absorber layer; b) EQE spectra of bulk heterojunction solar cells; c) Comparison of the PPDT2FBT-diode and the PPDT2FBT:PCBM-diode EQEs.

onset and the HOMO position of the donor. Data found for the studied polymers are added to the contour plot in different colors. One finds that several materials do have a performance potential around 10% PCE in accordance with reports published recently. Only for KP115 and PDCBT, the polymers with the highest lying HOMO level and the widest bandgap energy, moderate PCEs are predicted.
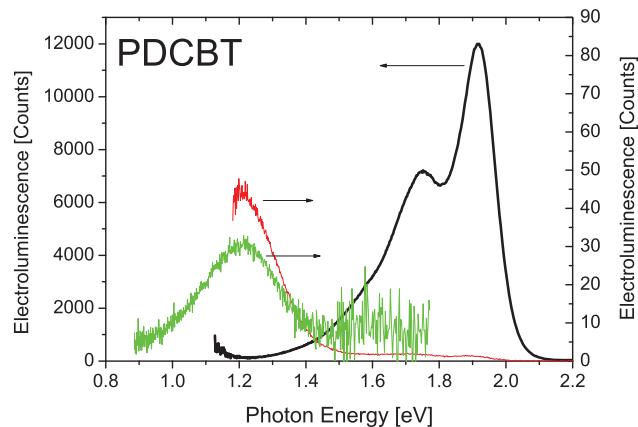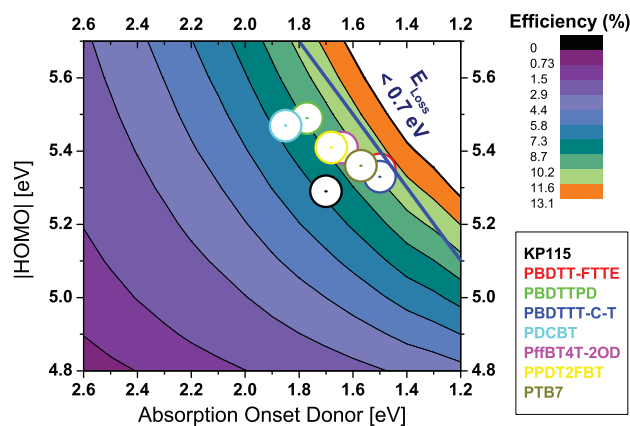

Figure 7. Contour plot showing the calculated energy-conversion efficiency (contour lines and colors) versus the absorption onset and the HOMO level of the donor polymer according to ref. [4] assuming an EQE and a FF of 70%; Dots in Figure 7 indicate the performance potential of the investigated polymers.

BHJ absorbers—the efficiency limit of OPV will be around 11% (Figure 7). Considering the performance gap found between small area hero devices fabricated in a lab and commercially manufactured modules made of the same absorber materials, module efficiencies around 10% are achievable under ideal conditions.[3] This efficiency may be sufficient for many niche market applications. Semitransparent OPVs—despite their low efficiency potential—may also be applied in BIPV. However, for a direct competition with state-of-the-art silicon PV—OPV hero cell PCEs in the range of 20% would be required.

There are several approaches available for incremental improvements of state of the art BHJ solar cells. The ideal absorber layer nanomorphology is still unknown and the power conversion efficiency of high-performance systems available today may be improved further by working on the molecular arrangement of donor and acceptor molecules in the absorber layer. A better morphology could lead to more efficient charge generation and charge transport. Antireflective coatings, high-performance substrates and electrodes with matched refractive indices and reduced reflection and absorption losses or advanced light trapping schemes based on nanophotonic or plasmonic structures could lead to enhanced light absorption.[46] Optimizing the chemical and structural purity of the organic semiconductors could lead to better performances as well. As discussed in detail for poly-3-hexyl-thiophene—the regioregularity and the molecular weight distribution of the polymer influences the processability, the nanomorphology and the charge transport in blend films.[47,48] Purer semiconductors may exhibit a reduced charge carrier recombination. In contrast to organic solar cells, the effect of surface recombination (SFR) is well understood in inorganic devices. Overcoming this loss by surface passivation and the implementation of a back-surface field (BSF) was one of the most important steps towards efficient silicon solar cells. There are only a few experimental studies available probing SFR in BHJs correlating performance losses to charge carrier recombination at the semiconductor—electrode interface.[49,50] Optimizing electrode materials could lead to better device performances but also to improved device stability. Considering all the efforts reported in the past decade on improving the power conversion efficiency of bulk heterojunction devices one expects only moderate improvements of the PCE upon further optimization.

For the best BHJs, the fill factor has already reached values close to the theoretical limit. The model proposed by Shockley and Queisser[51] predicts electrical fill factors in the range of 75%–85% when applied to an idealized donor–acceptor blend including a weakly absorbing CTS and reduced radiative recombination (Figure S5, Supporting Information). Adding typical electrical losses, FF between 70% and 80% are expected for BHJ.[52,53] Fill factors in this range have been reported for BHJ solar cells recently.[54]

Some optimization approaches discussed above may only be applicable to hero devices. That is ultrapure materials or advanced light managements structures may be too expensive to be used in commercial products. Nanophotonic concepts and slow processing steps may not be compatible to large area, high throughput production processes envisioned for OPVs.

For a radical increase of the performance potential of BHJ solar cells, absorber materials with new properties are required. As pointed out by Vandewal et al.,[31] Koster et al.,[33] and Gruber et al.,[32] donor–acceptor pairs with no CTS or strongly absorbing CTS should give higher power conversion efficiencies. These absorbers could even reach the Shockley–Queisser Limit when radiative recombination of charges is the only allowed recombination process in the material. That is semiconducting donor and acceptor materials with either extremely weak or extremely strong ground-state interaction are required leading either to no or a strongly absorbing CTS. In addition, the new donor–acceptor pairs need to exhibit high charge carrier generation and radiative recombination quantum yields. These insights should be used by chemists for the design of new semiconductors for OPV. Not only the bandgap and the energetic position of materials but also the interaction between the donor and acceptor component must be optimized. For next-generation materials, the arrangement of donor and acceptor moieties on the nanometer scale (nanomorphology) and the interaction between individual molecules needs to be controlled carefully. In this respect, advanced quantum-chemical calculations could be a very useful tool to identify promising candidates.

Improving the dielectric properties of organic semiconductor blends may also lead to significant PCE improvements. Koster et al.[33] argued that increasing the dielectric constant should reduce the exciton binding energy, the singlet–triplet energy splitting, the reorganization energy, the Coulomb attraction within the CT exciton, the geminate recombination back to the CT state, the bimolecular and trap-assisted recombination and space-charge effects. Implementing all these effects into a drift-diffusion model, the authors calculate an efficiency increase from 13% for $\varepsilon = 3\%$ to 21% for $\varepsilon = 10$. Several groups have reported the implementation of high-ε small molecule, nanoparticle additives or the introduction of polar substitutes to the organic semiconductor materials.[55–57] Device efficiencies were relatively low and the effect induced by the higher dielectric constant could hardly be distinguished from changes of the energetic levels in the donor–acceptor system, morphological or other changes induced by the added high-ε units. To which extent the dielectric constant, usually defined for macroscopic volumes, does influence electronic states with dimensions in the range of 1–2 nm in organic semiconductors is still controversial.[58]

Concepts for the third-generation PV[59] like tandem or multijunction solar cells, hot carrier cells, multiple electron–hole pairs per photon generation, impurity photovoltaic, multi-band cells, and thermophotovoltaic devices applied to OPVs could boost their power conversion efficiencies. Overcoming the thermalization losses of electrons and holes after photoexcitation and by extending the spectral range of solar cells, the third-generation PVs have a performance potential beyond the Shockley–Queisser Limit (33%) calculated for a classical single bandgap solar cell. In the case of organic solar cells—only a few third-generation concepts have been explored to date. Organic multijunction solar cells with efficiencies in the range of 10%–12% have been reported earlier.[60] However, as pointed out by Dennler et al.[61] —due the large V_{oc} loss of individual devices, stacking best BHJ solar cells on top of each other leads only to a moderate increase of the PCE. Similar to the situation discussed above—for highly efficient tandem cells new

semiconductors with optimized properties are required. There are reports supporting the idea that multiple electron–hole pair per photon generation is possible in OPVs. Singlet exciton fission, which transforms a molecular singlet excited state into two triplet states, which are converted into two electron–hole pairs, was reported in a pentacene/C_{60} solar cell. The reported effect was relatively small and did not result in high PCEs.[62] Today it is still unclear whether or not semiconductors used in BHJ solar cells are ideal candidates for the third-generation PV.

The discussion above suggests that new semiconductors based on new design rules are necessary for bringing BHJ-solar cells to a significantly higher performance level. Relating the chemical structure of donors and acceptors to the properties of the CTS will be essential. The resulting new materials could be the next generation of organic semiconductors with improved charge transport and higher radiative recombination quantum yields. These materials could also be useful for other organic electronic devices like detectors, transistors, or light emitting diodes.

In summary, eight high-performance conjugated polymers were investigated as donor materials in bulk heterojunction solar cells. The experiments revealed that all semiconductors showed typical losses and their ultimate power conversion efficiency limit when combined with the acceptor $PC_{60}BM$ is very well described by the model presented in AM2006. All BHJ solar cells show large V_{oc} losses, which limit their performance potential. The analysis suggests that the efficiency improvements observed over the last years were predominately driven by the synthesis of semiconductors with optimized band alignment and by the optimization of the nanomorphology of the absorber blend. Several approaches for higher power conversion efficiencies have been proposed. All of them require novel materials with improved electrical and optical properties. Developing the next-generation organic semiconductors for organic solar cells will be again a multidisciplinary research effort requiring the expertise of material chemists, spectroscopists and device engineers.

Experimental Section

Conjugated polymers used in this study were purchased or received from Solarmer (PBDTT-FTTE, PBDTTT-C-T), 1-Material (PDCBT, PffBT4T-2OD, PPDT2FBT, PTB7), Merck (KP115) and Prof. W. Maes, Hasselt University (PBDTTPD). The fullerene derivative $PC_{60}BM$ was provided by SolenneBV. All materials were used as received without further purification.

The electrochemical properties of all polymers were studied by electrochemical voltage spectroscopy (EVS). In EVS measurements, the voltage of an electrode is scanned at a rate that is slow enough to maintain the electrode close to thermodynamic equilibrium. Experiments were carried out on thin films at room temperature in a glove box under argon atmosphere using a computer-controlled potentiostat. The supporting electrolyte was tetrabutylammonium hexafluorophosphate (TBAPF6, 98%, Aldrich, ≈0.1 M) in anhydrous acetonitrile (Aldrich). Platinum foils were used as the working electrode (WE) as well as the counter electrode (CE). Polymer films were deposited on the WE by dropcasting. As a reference electrode (RE), a silver wire coated with AgCl was used. After each measurement, the RE was calibrated with ferrocene (oxidation potential E_0 = 400 mV versus normal hydrogen electrode (NHE)), and the potential axis was corrected to NHE according to the difference between E_0 (ferrocene) and the measured $E_{1/2}$ (ferrocene). For EVS measurements—initially the system was allowed to reach equilibrium at the starting potential $V = 0$ V. After that the potential was increased step-wise ($\Delta V = 20$ mV) and the resulting current was recorded for 30 s. The current was integrated for every voltage step to obtain ΔQ,

the amount of charge passing through the system. The oxidation onset potentials were determined as the position where ΔQ starts to differ from the baseline. Measured onset potentials were corrected to NHE and recalculated to electron volts versus vacuum level using a potential value of −4.75 eV for NHE.[63]

Different polymers were processed following the procedures described in the literature. Instead of spin-coating, blade coating was used to deposit the hole transport and the photoactive layers. Solar cells and light emitting diodes were prepared as small area (0.25 cm²) sandwich devices. The hole conductor PEDOT:PSS (CLEVIOS) was blade-coated at elevated temperature (75 °C) from an aqueous solution on a precleaned, patterned indium tin oxide (ITO)/glass substrate resulting in 60 nm thick layers. The semiconductor solutions were blade-coated on top of the PEDOT:PSS. To accelerate the drying of the wet film, layers were deposited on preheated substrates (70–90 °C). Further experimental details including layer thickness, used solvents and additives can be found in the Supporting Information. The devices were finalized by the deposition of a 0.8 nm thick LiF layer and a ≈100 nm aluminum layer as top electrodes. LiF and aluminum were thermally evaporated at a pressure <10^{-6} mbar. The geometry of the electrode was defined by a shadow mask. Device preparation was performed under ambient conditions, except for the evaporation of the top electrode. Devices were then encapsulated with a glass cover using a UV-curable epoxy sealant with a UV exposure time of ≈5 min. The finished solar cells with an active area of ≈0.25 cm² were tested on a LOT-QD solar simulator (LS0821). The radiation intensity was adjusted using a reference silicon diode to 100 mW cm⁻². External quantum efficiencies (EQEs) were recorded by using a lock-in amplifier (SR830, Stanford Research Systems) and a Jaissle 1002 potentiostat functioning as a preamplifier. The potentiostat operated in the two-electrode configuration is a high-performance current amplifier with a variable gain ranging from 10 to 10^8 V A⁻¹. The devices were illuminated by monochromatic light from a xenon lamp passing through a monochromator (Oriel Cornerstone) with typical intensities in the range of 0.1 to 10 µW. A filter wheel holding long-pass filters and a mechanical chopper was mounted between the Xenon lamp and the monochromator. Chopping frequencies in the range of 113–273 Hz were used. A calibrated silicon diode (Hamamatsu S2281) was used as a reference. UV–VIS absorption spectra of thin films were recorded using a double-beam UV–VIS spectrometer (Perkin Elmer 1050) equipped with an integrating sphere. Photoluminescence and electroluminescence spectra of various devices were measured using a Shamrock SR-303i monochromator and an Andor Peltier-cooled iDus Si-CCD (420-OE) and InGaAs detector array (DU420A). A white light lamp (Ocean Optics HL-2000) was used to determine the spectral response curves of the monochromator/detector systems. Samples were excited at 473 nm (5 mW) using a solid-state laser or a super-continuum light source (NKT EXB6) connected to a VIS-NIR SuperK Select Box. A set of long-pass filters was used to avoid any distortion of the recorded spectra by the laser light. Electroluminescence spectra were recorded while applying different potentials with a Keithley 2401.

Supporting Information

Supporting Information is available from the Wiley Online Library or from the author.

Acknowledgement

[1] Solar Efficiency Tables are published in the Journal Progress in Photovoltaics: Research and Applications.

[2] S. E. Shaheen, C. J. Brabec, N. S. Sariciftci, F. Padinger, T. Fromherz, J. C. Hummelen, *Appl. Phys. Lett.* **2001**, *78*, 841.

[3] M. A. Green, K. Emery, D. L. King, Y. Hishikawa, W. Warta, *Prog. Photovolt: Res. Appl.* **2006**, *14*, 455.

[4] M. C. Scharber, D. Mühlbacher, M. Koppe, P. Denk, C. Waldauf, A. J. Heeger, C. J. Brabec, *Adv. Mater.* **2006**, *18*, 789.

[5] *Informatics for Materials Science and Engineering: Data-Driven Discovery for Accelerated Experimentation and Application* (Ed: K. Rajan), Butterworth-Heinemann, Oxford **2013**.

[6] N. Blouin, A. Michaud, D. Gendron, S. Wakim, E. Blair, R. Neagu-Plesu, R. Belletete, G. Durocher, Y. Tao, M. Leclerc, *J. Am. Chem. Soc.* **2008**, *130*, 732.

[7] H. Zhou, L. Yang, W. You, *Macromolecules* **2012**, *45*, 607.

[8] J. Hachmann, R. Olivares-Amaya, S. Atahan-Evrenk, C. Amador-Bedolla, R. S. Sánchez-Carrera, A. Gold-Parker, L. Vogt, A. M. Brockway, A. Aspuru-Guzik, *J. Phys. Chem. Lett.* **2011**, *2*, 2241.

[9] J. Hachmann, R. Olivares-Amaya, A. Jinich, A. L. Appleton, M. Blood-Forsythe, L. R. Seress, C. Roman-Salgado, K. Trpte, S. Atahan-Evrenk, S. Er, S. Shrestha, R. Mondal, A. Sokolov, Z. Bao, A. Aspuru-Guzik, *Energy Environ. Sci.* **2014**, *7*, 698.

[10] N. E. Jackson, B. M. Savoie, T. J. Marks, L. X. Chen, M. A. Ratner, *J. Phys. Chem. Lett.* **2015**, *6*, 77.

[11] Y. Huang, E. J. Kramer, A. J. Heeger, G. C. Bazan, *Chem. Rev.* **2014**, *114*, 7006.

[12] T. Xu, L. Yu, *Mater. Today* **2014**, *17*, 11.

[13] H. Zhang, L. Ye, J. Hou, *Polym. Int.* **2015**, *64*, 957.

[14] S. H. Park, A. Roy, S. Beaupre, S. Cho, N. Coates, J. S. Moon, D. Moses, M. Leclerc, K. Lee, A. J. Heeger, *Nat. Photonics* **2009**, *3*, 297.

[15] J. Peet, J. Y. Kim, N. E. Coates, W. L. Ma, D. Moses, A. J. Heeger, G. C. Bazan, *Nat. Mater.* **2007**, *6*, 497.

[16] F. Padinger, R. Rittberger, N. S. Sariciftci, *Adv. Funct. Mater.* **2003**, *13*, 85.

[17] G. Li, Y. Yao, H. Yang, V. Shrotriya, G. Yang, Y. Yang, *Adv. Funct. Mater.* **2007**, *17*, 1636.

[18] M. A. Green, K. Emery, Y. Hishikawa, W. Warta, E. D. Dunlop, *Prog. Photovoltaics: Res. Appl.* **2015**, *23*, 805.

[19] J. Yao, T. Kirchartz, M. S. Vezie, M. A. Faist, W. Gong, Z. He, H. Wu, J. Troughton, T. Watson, D. Bryant, J. Nelson, *Phys. Rev. Appl.* **2015**, *4*, 014020.

[20] L. J. A. Koster, E. C. P. Smits, V. D. Mihailetchi, P. W. M. Blom, *Phys. Rev. B* **2005**, *72*, 085205.

[21] J. Hwang, A. Wan, A. Kahn, *Mater. Sci. Eng. R. Rep.* **2009**, *64*, 1.

[22] D. Veldman, S. C. J. Meskers, R. A. J. Janssen, *Adv. Funct. Mater.* **2009**, *19*, 1939.

[23] K. Vandewal, K. Tvingstedt, A. Gadisa, O. Inganäs, J. V. Manca, *Nat. Mater.* **2009**, *8*, 904.

[24] H. Kim, J. Y. Kim, S. H. Park, K. Lee, Y. Jin, J. Kim, H. Suh, *Appl. Phys. Lett.* **2005**, *86*, 183502.

[25] L. Goris, A. Poruba, L. Hod'ákova, M. Vaněček, K. Haenen, M. Nesládek, P. Wagner, D. Vanderzande, L. De Schepper, J. V. Manca, *Appl. Phys. Lett.* **2006**, *88*, 052113.

[26] J. J. Benson-Smith, L. Goris, K. Vandewal, K. Haenen, J. V. Manca, D. Vanderzande, D. D. C. Bradley, J. Nelson, *Adv. Funct. Mater.* **2007**, *17*, 451.

[27] M. A. Loi, S. Toffanin, M. Muccini, M. Forster, U. Scherf, M. Scharber, *Adv. Funct. Mater.* **2007**, *17*, 2111.

[28] K. Vandewal, A. Gadisa, W. D. Oosterbaan, S. Bertho, F. Banishoeib, I. Van Severen, L. Lutsen, T. J. Cleij, D. Vanderzande, J. V. Manca, *Adv. Funct. Mater.* **2008**, *18*, 2064.

[29] C. Deibel, T. Strobel, V. Dyakonov, *Adv. Mater.* **2010**, *22*, 4097.

[30] U. Rau, *Phys. Rev. B* **2007**, *76*, 085303.

[31] K. Vandewal, K. Tvingstedt, O. Ingan, *Quantum Efficiency in Complex Systems, Part II – From Molecular Aggregates to Organic Solar Cells, Vol. 85*, Academic Press, Elsevier, New York, USA **2011**, pp. 261.

[32] M. Gruber, J. Wagner, K. Klein, U. Hörmann, A. Opitz, M. Stutzmann, W. Brütting, *Adv. Energy Mater.* **2012**, *2*, 1100.

[33] L. J. A. Koster, S. E. Shaheen, J. C. Hummelen, *Adv. Energy Mater.* **2012**, *2*, 1246.

[34] Y. Liu, J. Zhao, Z. Li, C. Mu, W. Ma, H. Hu, K. Jiang, H. Lin, H. Ade, H. Yan, *Nat. Commun.* **2014**, *5*, 5293.

[35] S. Zhang, L. Ye, W. Zhao, D. Liu, H. Yao, J. Hou, *Macromolecules* **2014**, *47*, 4653.

[36] Z. He, B. Xiao, F. Liu, H. Wu, Y. Yang, S. Xiao, C. Wang, T. P. Russell, Y. Cao, *Nat. Photonics* **2015**, *9*, 174.

[37] J. Peet, L. Wen, P. Byrne, S. Rodman, K. Forberich, Y. Shao, N. Drolet, R. Gaudiana, G. Dennler, D. Waller, *Appl. Phys. Lett.* **2011**, *98*, 043301.

[38] E. T. Hoke, K. Vandewal, J. A. Bartelt, W. R. Mateker, J. D. Douglas, R. Noriega, K. R. Graham, J. M. J. Fréchet, A. Salleo, M. D. McGehee, *Adv. Energy Mater.* **2013**, *3*, 220.

[39] L. Huo, S. Zhang, X. Guo, F. Xu, Y. Li, J. Hou, *Angew. Chem. Int. Ed.* **2011**, *50*, 9697.

[40] M. Zhang, X. Guo, W. Ma, H. Ade, J. Hou, *Adv. Mater.* **2014**, *26*, 5880.

[41] T. L. Nguyen, H. Choi, S.-J. Ko, M. A. Uddin, B. Walker, S. Yum, J.-E. Jeong, M. H. Yun, T. J. Shin, S. Hwang, J. Y. Kim, H. Y. Woo, *Energy Environ. Sci.* **2014**, *7*, 3040.

[42] Z. He, C. Zhong, S. Su, M. Xu, H. Wu, Y. Cao, *Nat. Photonics* **2012**, *6*, 593.

[43] A. H. Thompson, *Phys. Rev. Lett.* **1978**, *40*, 1511.

[44] D. Di Nuzzo, G.-J. A. H. Wetzelaer, R. K. M. Bouwer, V. S. Gevaerts, S. C. J. Meskers, J. C. Hummelen, P. W. M. Blom, R. A. J. Janssen, *Adv. Energy Mater.* **2013**, *3*, 85.

[45] W. Li, K. H. Hendriks, A. Furlan, M. M. Wienk, R. A. J. Janssen, *J. Am. Chem. Soc.* **2015**, *137*, 2231.

[46] V. E. Ferry, A. Polman, H. A. Atwater, *ACS Nano* **2011**, *5*, 10055.

[47] M. Koppe, C. J. Brabec, S. Heiml, A. Schausberger, W. Duffy, M. Heeney, I. McCulloch, *Macromolecules* **2009**, *42*, 4661.

[48] Y. Kim, S. Cook, S. M. Tuladhar, S. A. Choulis, J. Nelson, J. R. Durrant, D. D. C. Bradley, M. Giles, I. McCulloch, C.-S. Ha, M. Ree, *Nat. Mater.* **2006**, *5*, 197.

[49] J. Reinhardt, M. Grein, C. Bühler, M. Schubert, U. Würfel, *Adv. Energy Mater.* **2014**, *4*, 1400081.

[50] S. Wheeler, F. Deledalle, N. Tokmoldin, T. Kirchartz, J. Nelson, J. R. Durrant, *Phys. Rev. Appl.* **2015**, *4*, 024020.

[51] W. Shockley, H. J. Queisser, *J. Appl. Phys.* **1961**, *32*, 510.

[52] J. D. Servaites, M. A. Ratner, T. J. Marks, *Appl. Phys. Lett.* **2009**, *95*, 163302.

[53] J. A. Bartelt, D. Lam, T. M. Burke, S. M. Sweetnam, M. D. McGehee, *Adv. Energy Mater.* **2015**, *5*, 15.

[54] L. Huo, T. Liu, B. Fan, Z. Zhao, X. Sun, D. Wei, M. Yu, Y. Liu, Y. Sun, *Adv. Mater.* **2015**, *27*, 6969.

[55] S. Y. Leblebici, T. L. Chen, P. Olalde-Velasco, W. Yang, B. Ma, *ACS Appl. Mater. Interfaces* **2013**, *5*, 10105.

[56] P. Yang, M. Yuan, D. F. Zeigler, S. E. Watkins, J. A. Lee, C. K. Luscombe, *J. Mater. Chem. C* **2014**, *2*, 3278.

[57] A. Lefrançois, B. Luszczynska, B. Pepin-Donat, C. Lombard, B. Bouthinon, J.-M. Verilhac, M. Gromova, J. Faure-Vincent, S. Pouget, F. Chandezon, S. Sadki, P. Reiss, *Sci. Rep.* **2015**, *5*, 7768.

[58] P. T. van Duijnen, H. D. de Gier, R. Broer, R. W. A. Havenith, *Chem. Phys. Lett.* **2014**, *615*, 83.

[59] M. A. Green, *Third Generation Photovoltaics*, Springer-Verlag, Berlin/Heidelberg **2006**, pp. 172.

[60] J. You, L. Dou, K. Yoshimura, T. Kato, K. Ohya, T. Moriarty, K. Emery, C.-C. Chen, J. Gao, G. Li, Y. Yang, *Nat. Commun.* **2013**, *4*, 1446.

[61] G. Dennler, M. C. Scharber, T. Ameri, P. Denk, K. Forberich, C. Waldauf, C. J. Brabec, *Adv. Mater.* **2008**, *20*, 579.

[62] D. N. Congreve, J. Lee, N. J. Thompson, E. Hontz, S. R. Yost, P. D. Reusswig, M. E. Bahlke, S. Reineke, T. van Voorhis, M. A. Baldo, *Science* **2013**, *340*, 334.

[63] R. Kötz, H. Neff, K. A. Müller, *J. Electroanal. Chem. Interfacial Electrochem.* **1986**, *215*, 331.